Available online at www.sciencedirect.com
ScienceDirect
Thermochimica Acta 454 (2007) 128–134
thermochimica acta
www.elsevier.com/locate/tca

Thermal conductivities of solid and liquid phases in Pb–Cd and Sn–Zn binary eutectic alloys

B. Saatçi *, N. Maraşlı, M. Gündüz

Department of Physics, Faculty of Arts & Sciences, Erciyes University, Kayseri, Turkey

Received 6 December 2006; received in revised form 28 December 2006; accepted 9 January 2007
Available online 17 January 2007

Abstract

The thermal conductivities of the Pb solution (Pb–3.3 wt.% Cd), the Cd solution (Cd–0.25 wt.% Pb), the Sn solution (Sn–1 wt.% Zn), the eutectic Pb–Cd (Pb–17.4 wt.% Cd) and the eutectic Sn–Zn (Sn–8.9 wt.% Zn) were measured with a radial heat flow apparatus up to eutectic temperature, T_E. The thermal conductivity ratios of the eutectic liquid phase to the eutectic solid phase, R for the Pb–Cd and Sn–Zn binary alloys were found with a Bridgman type directional solidification apparatus at T_E. Thus, the thermal conductivities of the eutectic liquid phases, κ_L, for the Pb–Cd and Sn–Zn eutectic binary alloys were obtained by using the values of κ_S and R at their eutectic temperature. Finally, the results have been compared with previous experimental values for binary alloys and pure materials.

Keywords: Thermal conductivity; Radial heat flow; Directional solidification; Pb–Cd alloy; Sn–Zn alloy

1. Introduction

The thermal conductivity, κ, is one of the main fundamental properties of materials such as density, melting point, entropy, resistance, and crystal structure parameters. Although the value of κ for pure materials was obtained theoretically and experimentally, there are not enough information and data available about the thermal conductivity of alloys. The values of κ for alloys change, as in pure materials, not only with temperature but also it changes by compositions of the materials. Many attempts have been made to determine the thermal conductivity values of solid and liquid phases in various materials by using different methods [1–6]. One of the common techniques for measuring the thermal conductivity of solids is the radial heat flow method and it is based upon specimen geometry; i.e. cylindrical or spherical. The cylindrical radial heat flow method uses a specimen in the form of a right circular cylinder with a coaxial central hole that contains either a heater or a sink depending on whether the described heat flow direction is to be radially outward or inward [1]. Temperatures within the specimen are measured by thermocouples. This method was first used for measuring the thermal conductivity of solids for pure materials by Callender and Nicolson [2] then this method was used by Niven [3] and Powell [4]. A review of radial heat flow methods was presented by McElroy and Moore [6].

Consider a cylindrical specimen heated by a heating element along the axis at the center of the specimen. It is assumed that the heat flow, the temperatures at radii r_1 and r_2, T_1 and T_2, respectively are known and are constant. At the steady-state conditions, thermal conductivity of solid can be determined by using appropriate boundary conditions with Fourier's law for the radial heat flow, and the temperature gradients are given as

$$\left(\frac{dT}{dr}\right)_S = -\frac{Q}{2\pi r l \kappa_S} \tag{1}$$

where Q is the total input power from the center of the specimen, l the length of the heating element, κ_S the thermal conductivity of the solid phase, and r is the distance from the centre.

Integration of Eq. (1) for the radial heat flow gives

$$\kappa_S = \frac{1}{2\pi l} \ln\left(\frac{r_2}{r_1}\right) \frac{Q}{T_1 - T_2} \tag{2}$$

* Corresponding author. Tel.: +90 352 437 49 01/33 102; fax: +90 352 437 49 33.
E-mail address: bayender@erciyes.edu.tr (B. Saatçi).

0040-6031/$ – see front matter © 2007 Elsevier B.V. All rights reserved.
doi:10.1016/j.tca.2007.01.009

or

$$\kappa_S = a_0 \frac{Q}{T_1 - T_2} \quad (3)$$

where $a_0 = \ln(r_2/r_1)/2\pi l$ is an experimental constant, r_1 and r_2 the fixed distances from the centre of the sample ($r_2 > r_1$), and T_1 and T_2 are the temperatures at the fixed positions r_1 and r_2, respectively. If the value of Q, r_1, r_2, l, T_1 and T_2 can be accurately measured for the well-characterized sample, then reliable κ_S values can be evaluated provided that the vertical temperature variations is minimum or zero.

The goal of the present work is to experimentally determine the thermal conductivities of the solid phases for the Pb solution (Pb–3.3 wt.% Cd), the Cd solution (Cd–0.25 wt.% Pb), the Sn solution (Sn–1 wt.% Zn), the eutectic Pb–Cd (Pb–17.4 wt.% Cd) and the eutectic Sn–Zn (Sn–8.9 wt.% Zn) from 50 °C to their melting temperatures with a radial heat flow apparatus and the thermal conductivity ratios of the liquid phases to the solid phases for the Pb–17.4 wt.% Cd and Sn–8.9 wt.% Zn eutectic alloys with a Bridgman type directional growth apparatus to calculate the thermal conductivities of the liquid eutectic Pb–Cd and Sn–Zn alloys at their melting temperature.

2. Experimental procedure

2.1. Measurement of thermal conductivity of solid phases

In present work, the radial heat flow apparatus was chosen to determine the thermal conductivity of solids, because of its symmetrical characteristics. A radial heat flow apparatus, originally designed by Gündüz and Hunt [7,8] and modified by Maraşlı and Hunt [9] were used to experimentally determine the thermal conductivity of solid phases. More details of the apparatus are described in Refs. [7–12]. The radial heat flow apparatus consists of a central heating element and a water cooling jacket. The central heating element was a 1.7 mm Kanthal A-1 wire inside a thin walled alumina tube and was used to heat specimen from center. The water cooling jacket is made of stainless steel and was used to cool the outside of the specimen. To get radial heat flow, the specimen was heated from the centre and the out side of the specimen was kept cool with the water cooling jacket. The temperature gradient on the specimen could be modified by placing different materials into the gap between the specimen and the water cooling jacket.

The crucible was made as symmetrical as possible to ensure that the isotherms were almost parallel to the central axis. The crucible consisted of three parts, a 170 mm length of cylindrical bore, the top and the bottom lids. The lids were pushed into the cylindrical bore. The cylindrical bore was 30 mm ID (inner diameters) × 40 mm OD (outer diameters) × 170 mm long. The top and bottom lids were made as symmetrical as possible. The top lid had four air or feeding holes, one vertical thermocouple hole and one central hole for the alumina tube. The bottom lid had five holes, three holes for the fixed thermocouples (one of them for the control unit, two others for measurement thermocouples), one for the vertical thermocouple and one for the central alumina tube. The control unit thermocouple and one of the measurement thermocouples were placed 1–2 mm away form the central alumina tube. The vertical (movable) and one of the measurements thermocouple holes were drilled 10–12 mm away from the centre.

Approximately 1×10^{-4} m^3 of metal was melted in a graphite crucible using the vacuum melting furnace. This amount of alloy was sufficient to produce an ingot of approximately 150 mm long and 30 mm in diameter. Just before use, the metals (Pb, Cd, Sn and Zn) were chemically cleaned and dried. The right amount of metal was melted under the vacuum approximately 50 °C above the melting point of the alloys. After the metal had melted the molten metal was stirred with a graphite rod and mixed with a graphite plunger. The molten metal was poured into the graphite crucible held in a specially constructed casting furnace at approximately 50 °C above the melting temperature of the alloys. The molten alloy was then directionally solidified from the bottom to the top to ensure that the crucible was completely filled. The sample was then taken out from the hot filling furnace and placed into the radial heat flow apparatus.

The specimen was heated from the center using a single heating wire (170–220 mm length and 1.7 mm in diameter, Kanthal A-1) in steps of 50 °C up to 10 °C below the melting temperature and the outside of the specimen was kept cool with the water cooling jacket to get a radial temperature gradient. The length of the central heating wire was chosen to be slightly longer than the length of the specimen to make the vertical isotherms parallel to the axis. The gap between the cooling jacket and the specimen was filled with free running sand or graphite dust to get a large radial temperature gradient on the specimen. The larger radial temperature gradient is desired to increase the experimental sensitivity for the solid phase thermal conductivity measurements. The temperature of the specimen was controlled with a Euroterm 905S type controller and the temperature in the specimen was stable to ±0.1 °C for at least 2 h. At the steady state, the total input power and the temperatures of the stationary thermocouples were recorded with Hewlett Packard 34401 type multimeters and a data logger. The vertical temperature gradient must be smaller than the horizontal gradient at the position of the thermocouples for cylindrical heat flow. The vertical isotherm for each setting was made parallel to the axis at the measurement region by moving the central heater up and down, as shown in Fig. 1. When all the desired parameters and the temperature measurements were completed the specimen was left to cool to the room temperature.

For the measurement of the r_1 and r_2, the specimen was cut near the temperature measurement point. The distances of the fixed thermocouples from the center were measured with an Olympus BH2 optical microscope to an accuracy of ±10 μm. The transverse and longitudinal sections of the specimen were examined for the porosity, crack and casting defects to make sure that these would not introduce any errors to the measurements. All the values are given in Tables 1 and 2. In Figs. 2 and 3, the values of the thermal conductivity of solid phase, κ_S, at the melting temperature, T_E is obtained by extrapolating the thermal conductivity versus temperature curves to the melting temperature. The thermal conductivity of the solid phase depends on the composition as well as the temperature as shown in Figs. 2 and 3.

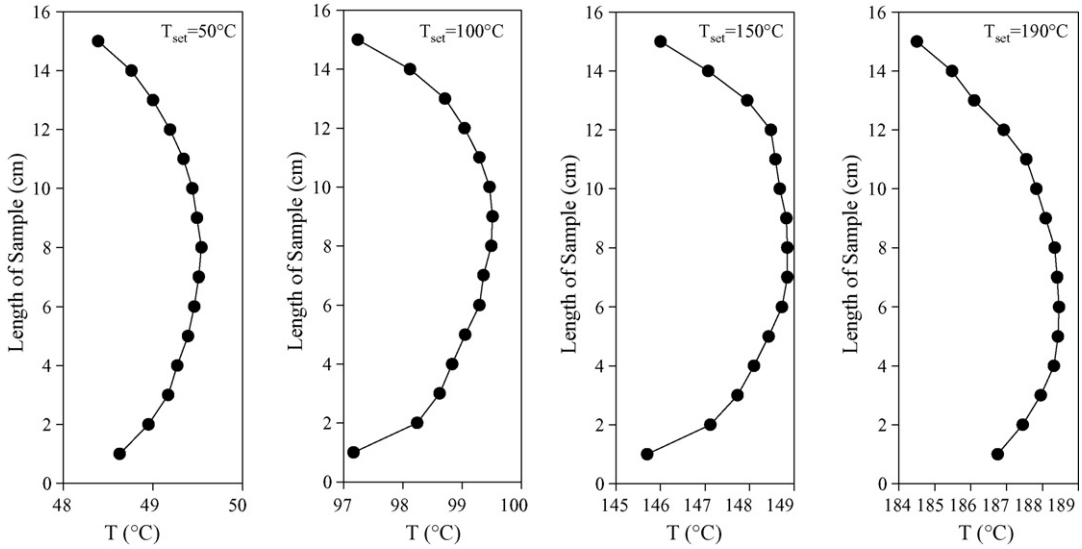

Fig. 1. Typical vertical temperature variations in the specimen at different setting temperatures.

2.2. Thermal conductivity ratio of liquid phase to solid phase

It is not possible to measure the thermal conductivity of liquid phase with the radial heat flow apparatus since a thick liquid layer (10 mm) is required. A layer of this size would certainly have led to convection. If the ratio of thermal conductivity of the liquid phase to solid phase is known and the thermal conductivity of the solid phase is measured at the eutectic (or melting) temperature, the thermal conductivity of the liquid phase can then be evaluated. The thermal conductivity ratio can be obtained during directional growth with the Bridgman type growth apparatus. The heat flow away from the interface through the solid phase must balance that liquid phase plus the latent heat generated at

Table 1
Experimental data for the thermal conductivity determination of the (a) Pb–17.4 wt.% Cd eutectic alloy, (c) Pb–3.3 wt.% Cd alloy, and (d) Cd–0.25 wt.% Pb alloy

T (°C)	Q (W)	T_1 (°C)	T_2 (°C)	$\Delta T = T_1 - T_2$ (°C)	κ_S (W/K m)
(a) Pb–17.4 wt.% Cd eutectic alloy[a]					
50.00	17.58	48.31	48.00	0.31	62.77
100.00	57.60	98.05	96.85	1.20	53.14
150.00	99.27	150.92	148.45	2.47	44.49
200.00	128.50	200.09	196.53	3.56	39.96
240.00	175.63	240.34	235.12	5.22	37.25
249.25	–	–	–	–	35.94[b]
(c) Pb–3.3 wt.% Cd alloy[c]					
50.00	13.56	49.31	49.00	0.31	38.36
100.00	38.11	99.72	98.79	0.93	35.94
150.00	70.21	151.14	149.14	2.00	30.79
200.00	107.71	201.28	198.17	3.11	30.37
240.00	143.62	240.78	236.23	4.55	27.68
249.25	–	–	–	–	27.60[b]
(d) Cd–0.25 wt.% Pb alloy[d]					
50.00	22.63	49.46	49.23	0.23	105.18
100.00	42.67	99.97	99.44	0.53	86.06
150.00	78.44	152.57	151.39	1.18	71.06
200.00	114.87	202.37	200.62	1.77	69.38
240.00	158.64	241.30	238.53	2.77	61.22
249.25	–	–	–	–	62.60[b]

[a] $r_1 = 0.25 \pm 0.001$ cm, $r_2 = 0.95 \pm 0.001$ cm, $l = 19.2 \pm 0.05$ cm, $a_0 = 0.01107\ \text{cm}^{-1}$.
[b] Obtained from the extrapolating of the κ–T curves.
[c] $r_1 = 0.27 \pm 0.001$ cm, $r_2 = 0.80 \pm 0.001$ cm, $l = 19.7 \pm 0.05$ cm, $a_0 = 0.00877\ \text{cm}^{-1}$.
[d] $r_1 = 3.1 \pm 0.001$ cm, $r_2 = 10.6 \pm 0.001$ cm, $l = 18.3 \pm 0.05$ cm, $a_0 = 0.01069\ \text{cm}^{-1}$.

Table 2
Experimental data for the thermal conductivity determination of (a) Sn–8.9 wt.% Zn eutectic alloy and (b) Sn–1 wt.% Zn alloy

T (°C)	Q (W)	T_1 (°C)	T_2 (°C)	$\Delta T = T_1 - T_2$ (°C)	κ_S (W/K m)
(a) Sn–8.9 wt.% Zn eutectic alloy[a]					
50	12.84	49.36	49.50	0.14	86.39
100	44.08	98.78	99.29	0.51	81.42
150	73.84	150.76	151.64	0.88	79.04
190	103.28	189.95	191.24	1.29	75.42
199	–	–	–	–	74.74[b]
(b) Sn–1 wt.% Zn alloy[c]					
50	14.22	48.48	48.33	0.15	78.49
100	42.66	100.41	99.93	0.48	73.59
150	75.94	150.43	149.49	0.94	66.89
190	103.02	191.28	190.08	1.20	71.08
199	–	–	–	–	66.65[b]

[a] $r_1 = 0.23 \pm 0.001$ cm, $r_2 = 0.76 \pm 0.001$ cm, $l = 20.2 \pm 0.05$ cm, $a_0 = 0.00942$ cm^{-1}.
[b] Obtained from the extrapolating of the κ–T curves.
[c] $r_1 = 0.41 \pm 0.001$ cm, $r_2 = 1.16 \pm 0.001$ cm, $l = 20 \pm 0.05$ cm, $a_0 = 0.00828$ cm^{-1}.

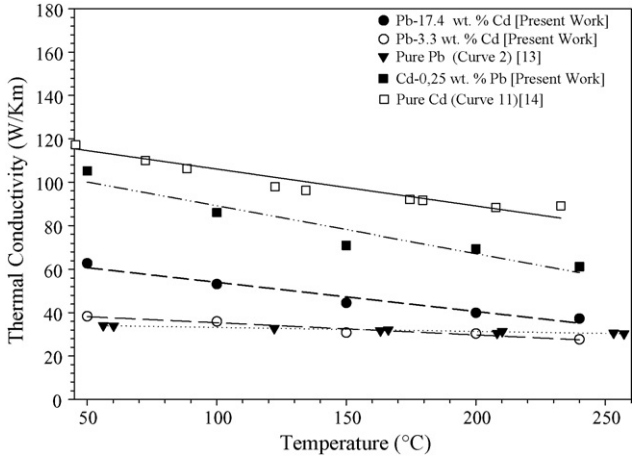

Fig. 2. Thermal conductivity variations with temperature for Pb–Cd alloys, pure Pb [13] and pure Cd [14].

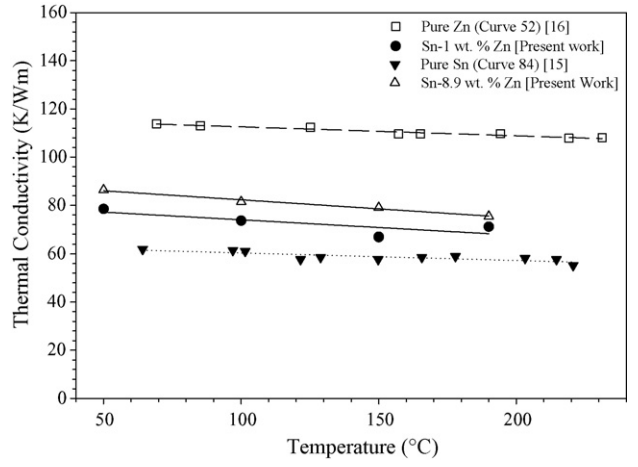

Fig. 3. Thermal conductivity variations with temperature for Sn–Zn alloy, pure Sn [15] and pure Zn [16].

the interface, i.e. [17]:

$$VL = \kappa_S G_S - \kappa_L G_L \tag{4}$$

where V is the growth rate, L the latent heat, G_S and G_L the temperature gradients in the solid and liquid, respectively and κ_S and κ_L are the thermal conductivities of the solid and the liquid phases, respectively. For very low growth rates $VL \ll \kappa_S G_S$, so that the conductivity ratio, R is given by

$$R = \frac{\kappa_L}{\kappa_S} = \frac{G_S}{G_L} \tag{5}$$

If the right hand side of Eq. (5) is obtained and the value of κ_S is measured, then the liquid thermal conductivity can be evaluated from Eq. (5) [7–12].

In the present work, the thermal conductivity ratio of liquid phase to solid phase, R, was obtained in a directional growth apparatus (Bridgman type) [18]. A directional growth apparatus which was first constructed by McCartney [19] was used to determine the thermal conductivity ratio $R = \kappa_L/\kappa_S$. A thin walled graphite crucible was produced by drilling out a graphite rod of 6.35 mm outer diameter and with a 4 mm bore. Pb–Cd and Sn–Zn alloys were prepared in a vacuum furnace [7–12]. After stirring, the molten metal was poured into thin walled graphite crucibles and the molten alloy was then directionally frozen from bottom to top to ensure that the crucible was completely full. After that the specimen was then placed in the directional growth apparatus, the directional growth apparatus was flushed with argon before heating the furnace and the specimen was heated to 100 °C over the melting temperature of the alloy. The specimen was then left to reach the thermal equilibrium for at least 2 h. The temperature in the specimen was measured with an insulated 0.5 mm K-type thermocouple. When the specimen temperature stabilized, the directional growth was begun by turning on the motor and the temperature change with time was recorded by a data logger (TC-08 type data logger).

The conductivity ratio was evaluated from the change in the slope of the temperature versus time curves. From the temperature versus time curves, the slope of the liquid and solid phases can be written as

$$\left(\frac{dT}{dt}\right)_L = \left(\frac{dT}{dx}\right)_L \left(\frac{dx}{dt}\right)_L = G_L V_L \tag{6}$$

and

$$\left(\frac{dT}{dt}\right)_S = \left(\frac{dT}{dx}\right)_S \left(\frac{dx}{dt}\right)_S = G_S V_S \tag{7}$$

$V_L = V_S$ then from Eqs. (6) and (7), the thermal conductivity ratio can be written as

$$R = \frac{\kappa_L}{\kappa_S} = \frac{G_S}{G_L} = \frac{(dT/dt)_S}{(dT/dt)_L} \tag{8}$$

where $(dT/dt)_S$ and $(dT/dt)_L$ values were directly measured from the curves of the temperature versus time graphs as shown in Figs. 4 and 5. Then the values of κ_L were obtained from Eq. (5) by using the measured values of κ_S and R and are given in Table 3.

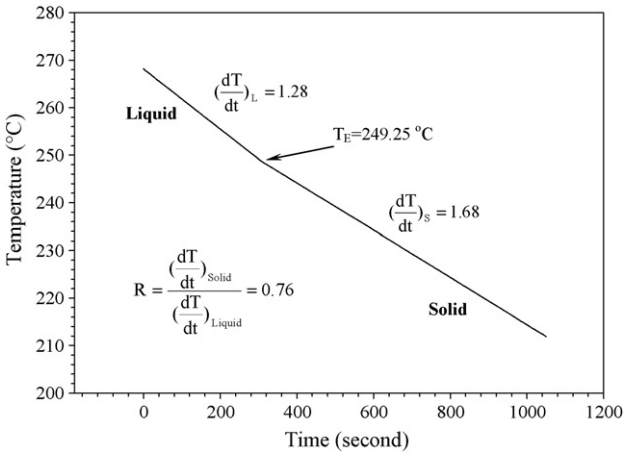

Fig. 4. Temperature vs. time for Pb–17.4 wt.% Cd eutectic alloy.

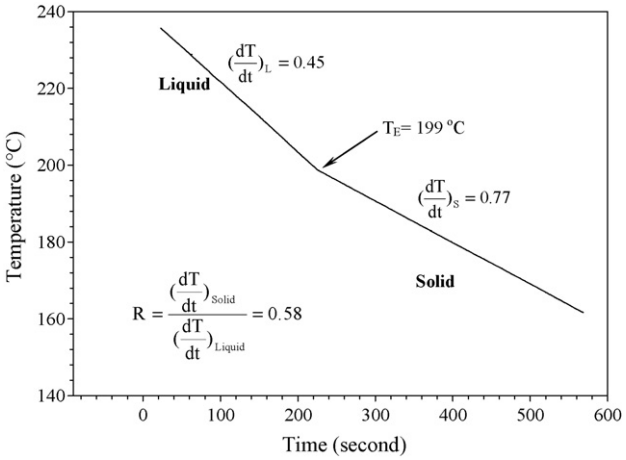

Fig. 5. Temperature vs. time for Sn–8.9 wt.% Zn eutectic alloy.

3. Results and discussions

3.1. Thermal conductivity of solid phase

The thermal conductivities of the Pb solution, the Cd solution, the Sn solution, the eutectic Pb–Cd and the eutectic Sn–Zn were measured with a radial heat flow apparatus. The thermal conductivities of the solid phase, κ_S, versus temperature for Pb–Cd and Sn–Zn alloys are shown in Figs. 2 and 3, respectively. As can be seen from Figs. 2 and 3, the values of κ_S at the eutectic temperature are obtained by extrapolating the κ–T curves to the melting temperature. A comparison of our results with values of κ_S found in the literature is also given in Table 3, and a good agreement is observed.

The estimated experimental error in the measurement of κ_S is sum of the fractional uncertainty of the measurements of power, temperature difference, length of heating wire and thermocouples positions which can be expressed as

$$\left|\frac{\Delta\kappa_S}{\kappa_S}\right| = \left|\frac{\Delta Q}{Q}\right| + \left|\frac{\Delta T^*}{T_1 - T_2}\right| + \left|\frac{\Delta l}{l}\right| + \left|\frac{\Delta r_1}{r_1}\right| + \left|\frac{\Delta r_2}{r_2}\right| \quad (9)$$

3.1.1. Fractional uncertainty in the power measurement

The input power is expressed as

$$Q = \frac{V_{sh}}{R_{sh}} V_h \quad (10)$$

where V_{sh} and V_h are the potential differences between the ends of the shunt and the ends of the central heating wire and R_{sh} is the shunt resistance. The fractional uncertainty in the power measurement can be expressed as

$$\left|\frac{\Delta Q}{Q}\right| = \left|\frac{\Delta R_{sh}}{R_{sh}}\right| + \left|\frac{\Delta V_h}{V_h}\right| + \left|\frac{\Delta V_{sh}}{V_{sh}}\right| \quad (11)$$

The potential differences between the ends of the shunt and the ends of the central heating wire and the shunt resistance were measured with a Hewlett-Packard 34401-A multimeter to an accuracy of ±1%. Thus the total fractional uncertainty in power measurement is about 3%.

3.1.2. The fractional uncertainty in the measurement of heating wire's length, l, and the fixed distances (r_1, r_2)

The length of heating wire was measured to an accuracy of ±0.5 mm and the fixed distances (r_1, r_2) were measured with an optical microscope to an accuracy of ±10 μm. Therefore, the total fractional uncertainty for measuring the heating wire's length and the fixed distances is less than 1%.

3.1.3. Fractional uncertainty in the measurement of $\Delta T = T_1 - T_2$

The measurements thermocouples were calibrated by detecting the melting point of alloy as shown in Fig. 6. It can be seen from Fig. 6, the difference between two thermocouples reading, ΔT^* at 175 °C was measured to be an accuracy of ±0.1–0.2 K. The temperature difference between the two thermocouples, ΔT at above 100 °C was 2–6 °C. Thus the uncertainty in the temperature measurement at high temperature (above 100 °C) is about 10%.

Therefore, the total fractional uncertainty in the measurements of thermal conductivity of solid phase is about 13%.

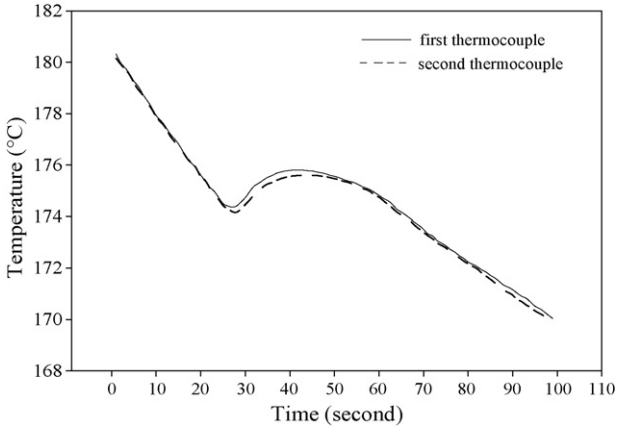

Fig. 6. Thermocouples calibration by detecting melting temperature.

Table 3
Thermal conductivities of the solid and the liquid phases at their eutectic melting temperatures of binary alloys

System	Phases	T_E (°C)	κ (W/K m)
Pb–Cd	Solid Pb (Pb–3.3 wt.% Cd)	249.25	27.60 ± 3.59 (present study)
	Solid Pb–Cd eutectic (Pb–17.4 wt.% Cd)	35.94 ± 4.67 (present study)	
	Solid Cd (Cd–0.25 wt.% Pb)	62.60 ± 8.14 (present study)	
	Liquid Pb–Cd eutectic (Pb–17.4 wt.% Cd)	28.10 ± 3.65 (present study)	
Sn–Zn	Solid Sn (Sn–1 wt.% Zn)	199.00	52.60 ± 6.84 (present study)
	Solid Sn–Zn eutectic (Sn–8.9 wt.% Zn)	35.74 ± 4.65 (present study)	
	Liquid Sn–Zn eutectic (Sn–8.9 wt.% Zn)	21.10 ± 2.74 (present study)	
Pb–Sn	Solid Pb (Pb–19 wt.% Sn)	183.00	35.9 [7]
	Solid Pb–Sn eutectic (Pb–61.9 wt.% Sn)	40.1 [7]	
	Solid Sn (Sn–2.5 wt.% Pb)	52.3 [7]	
	Liquid Pb–Sn eutectic (Pb–61.9 wt.% Sn)	32.2 [7]	
Pb–10 wt.% Sn	Solid Pb (Pb–10 wt.% Sn)	183.00	29.7 [25]
	Liquid Pb–Sn eutectic (Pb–61.9 wt.% Sn)	15.4 [25]	
Cd–Zn	Solid Cd (Cd–2.95 wt.% Zn)	266.00	86 [11]
	Solid Cd–Zn eutectic (Cd–17.4 wt.% Zn)	78 [11]	
	Solid Zn (Zn–1.3 wt.% Cd)	77 [11]	
	Liquid Cd–Zn eutectic (Cd–17.4 wt.% Zn)	60 [11]	
Cd–Bi	Solid Cd (Cd–0.05 wt.% Bi)	145.70	100.55 [23]
	Solid Cd–Bi eutectic (Cd–60.3 wt.% Bi)	12.46 [20]	
	Liquid Cd–Bi eutectic (Cd–60.3 wt.% Bi)	10.06 [20]	
Cd–Sn	Solid Sn (Sn–5.83 wt.% Cd)	177.00	53 [21]
	Solid Cd–Sn eutectic (Cd–67.75 wt.% Sn)	59.8 [21]	
	Liquid Cd–Sn eutectic (Cd–67.75 wt.% Sn)	44 [21]	
Bi–50 wt.% Sn	Solid	138.90	60 [26]
	Sn	30 [26]	
	(Bi–50 wt.%	32.5 [24]	
	Sn)		
Sn	Solid	138.90	59 [14]
	Sn	69.5 [15]	
Al–Zn	Solid Zn (Zn–16 wt.% Al)	380.00	133 [27]
	Solid Al–Zn eutectic (Zn–5 wt.% Al)	122 [27]	
	Liquid Al–Zn eutectic (Zn–5 wt.% Al)	108.6 [27]	
Zn–5 wt.% Al	Solid Zn (Zn–5 wt.% Al)	380.00	122 [22]
Zn–0.5 wt.% Al	Solid Zn (Zn–1 wt.% Al)	380.00	106.5 [22]
Mg–Zn	Solid Zn (Zn–0.15 wt.% Mg)	366.28	137.40 ± 6.9 [20]
	Liquid Mg–Zn eutectic (Mg–3 wt.% Zn)	107.20 ± 5.4 [20]	
Zn	Solid Zn	366.28	103.10 [16]

3.2. Thermal conductivity ratio of liquid phase to solid phase

The value of R can be evaluated from the ratio of the solid phase slope to the liquid phase slope. As can be seen from Figs. 4 and 5, the values of R for the eutectic Pb–Cd and the eutectic Sn–Zn alloys at their eutectic temperature are found to be $R = 0.76$ and 0.58, respectively, using a Bridgman type directional solidification apparatus. The thermal conductivities of the Pb solution, the Cd solution, the eutectic Pb–Cd alloys and the Sn solution, the eutectic Sn–Zn alloys at their eutectic temperature are measured to be 27.60 ± 3.59, 62.60 ± 8.14, 35.94 ± 4.67 W/K m for Pb–Cd alloys and 52.60 ± 6.84 and 35.74 ± 4.65 W/K m for Sn–Zn alloys, respectively. Also, the thermal conductivity of the liquid phase, κ_L, for the eutectic Pb–Cd and the eutectic Sn–Zn was determined to be 28.10 ± 3.65 and 21.10 ± 2.74 W/K m, respectively, from Eq. (8) using the values of κ_S and R. The evaluated values κ_S are also given in Table 3. As can be seen from Table 3, our experimental results are in good agreement with previous experimental results.

4. Conclusions

A radial heat flow apparatus were used to experimentally determine the thermal conductivities of the solid phases. The thermal conductivities of solid phases for the Pb solution, the Cd solution, the Sn solution, the eutectic Pb–Cd and eutectic Sn–Zn were measured with the radial heat flow apparatus from 50 °C to their melting temperature. The thermal conductivity ratios of liquid phase to solid phase for the eutectic Pb–Cd and for the eutectic Sn–Zn at their eutectic temperature were also measured

with a Bridgman type directional solidification apparatus and the thermal conductivity of liquid phases for the same alloys were also evaluated at their eutectic temperature using the values of κ_S and R. A comparison of our results with the previous work are shown in Table 3. A reasonable good agreement is obtained between the experimental values of the thermal conductivities, κ_S and κ_L, of the Pb solution, the Cd solution, the Sn solution, the eutectic Pb–Cd and the eutectic Sn–Zn alloys with the previous works.

Acknowledgments

This project was supported by Erciyes University Scientific Research Project Unit under contract no. 92-12-5. Authors would like to thank to Erciyes University Scientific Research Project Unit for their financial supports.

References

[1] Y.S. Touloukian, R.W. Powell, C.Y. Ho, P.G. Klemens, Thermal Conductivity, Metallic Elements and Alloys, Thermophysical Properties of Matter, vol. 1, Plenum, New York, 1970, pp. 3a–25a.
[2] H.L. Callender, J.T. Nicolson, Brt. Assoc. Adv. Sci. Rept. Ann. Meeting, vol. 418, 1897, p. 22.
[3] C. Niven, Proc. Roy. Soc. A 76 (1905) 34.
[4] R.W. Powell, Proc. Phys. Soc. 51 (1939) 407.
[5] M.F. Angel, Phys. Rev. 33 (1911) 411.
[6] D.L. McElroy, J.P. Moore, Thermal Conductivity, vol. 1, Academic Press, London, 1969, pp. 185 (Chapter 4).
[7] M. Gündüz, J.D. Hunt, Acta Mater. 33 (1985) 1651.
[8] M. Gündüz, J.D. Hunt, Acta Mater. 37 (1989) 1839.
[9] N. Maraşlı, J.D. Hunt, Acta Mater. 44 (1996) 1085.
[10] B. Saatçi, D.Phil. Thesis, Erciyes University, Turkey, 2000, p. 81.
[11] B. Saatçi, H. Pamuk, J. Phys.: Condens. Matter 18 (2006) 10143.
[12] B. Saatçi, M. Arı, M. Gündüz, F. Meydaneri, M. Bozoklu, S. Durmuş, J. Phys.: Condens. Matter 18 (2006) 10643.
[13] Y.S. Touloukian, R.W. Powell, C.Y. Ho, P.G. Klemens, Thermal Conductivity Metalic Elements and Alloys, vol. 1, 1970, pp. 185–191.
[14] Y.S. Touloukian, R.W. Powell, C.Y. Ho, P.G. Klemens, Thermal Conductivity Metalic Elements and Alloys, vol. 1, 1970, pp. 45–49.
[15] Y.S. Touloukian, R.W. Powell, C.Y. Ho, P.G. Klemens, Thermal Conductivity Metalic Elements and Alloys, vol. 1, 1970, pp. 405–408.
[16] Y.S. Touloukian, R.W. Powell, C.Y. Ho, P.G. Klemens, Thermal Conductivity Metalic Elements and Alloys, vol. 1, 1970, pp. 458–460.
[17] D.A. Porter, K.E. Easterling, Phase Transformations in Metals and Alloys, Van Nostrnad Reinhold Co. Ltd., UK, 1991, p. 204.
[18] E. Çadırlı, D.Phil. Thesis, Erciyes University, Turkey, 1997, p. 77.
[19] D.G. McCartney, D.Phil. Thesis, University of Oxford, UK, 1981, pp. 85–175.
[20] M. Erol, K. Keşlioğlu, R. Şahingöz, N. Maraşlı, Metal Mater. Int. 11 (5) (2005) 421.
[21] S. Çimen, M.Sc. Thesis, Erciyes University, Turkey, 2005, p. 74.
[22] K. Keşlioğlu, N. Maraşlı, Metall. Mater. Trans. A 35 (2004) 3665.
[23] K. Keşlioğlu, M. Erol, N. Maraşlı, M. Gündüz, J. Alloy Compd. 385 (2004) 207.
[24] B.P. Pashaev, Soviet Phys. Solid-State 38 (1962) 1773.
[25] S.N. Tewari, J. Crystal Growth 118 (1992) 183.
[26] S.R. Coriell, R.F. Boisvert, G.B. Mc Fadden, L.N. Brush, J.J. Favier, J. Crystal Growth 140 (1994) 139.
[27] K. Keşlioğlu, N. Maraşlı, Mater. Sci. Eng. A 369 (2004) 294.